Statistical Pattern Recognition
Final Project Report

# Maximum Likelihood Approximate Nearest Neighbor Method in Real-time Face Recognition

*Submitted in partial fulfillment of the degree*

Bachelor of Science
in
Software Engineering

Submitted by
Ali Gholami

Under the guidance of
Prof. Mohammad Rahmati


Department of Computer Engineering and Information Technology
Amirkabir University of Technology

Spring Semester 2018

**Abstract**

Image recognition is one of the fundamental tasks in computer vision. Modern face recognition which is one of the substantial subtasks of the image recognition, in most cases, uses *brute-force* nearest neighbor method to iterate through the reference faces database to find the desired identity of the input image. Nowadays, most of these methods extract feature maps of the images using Convolutional Neural Networks. In this project, we'll be using Convolutional Neural Networks to extract image feature maps. We'll also analyze the implementation process of the *Approximate Nearest Neighbor* method to find the best ID for the input image.

# Contents

# List of Figures

# Chapter 1

# Introduction

## 1.1 Motivation

One of the well-known issues of vision systems building, is a processing of large databases. Unfortunately, nearest neighbor (NN) rule and exhaustive search usually cannot be implemented in real-time applications[1]. To overcome these problems, we'll analyze some of the purposed methods in this this topic.

## 1.2 Recent Methods of Image Recognition in Large Scale Databases

In this section we'll take a brief look at the recent researches on image recognition systems and their improvements for large scale databases.

### 1.2.1 Approximate Nearest Neighbor Shape Indexing

This method relies on the rapid recovery of the nearest neighbors from the index. In high-dimensional databases, standard $k$-d tree search often performs poorly. having to examine a large fraction of the points in the space to find the exact nearest neighbor. However, a variant of this search which efficiently finds approximate neighbors will be used to limit the search time. The algorithm, which we have called Best Bin First (BBF) search, finds the nearest neighbor for a large fraction of queries, and finds a very good neighbor the remaining times [2].

### 1.2.2 Directed Enumeration Method

Directed enumeration method is proposed to improve image recognition performance. The method is applied with similarity measures which do not met metric properties. This method increases performance in 3 to 12 times in comparison with nearest neighbor. Recognition speed using *DEM* is increased when many neighbors are located at similar distances [3].

### 1.2.3 Directed Enumeration Alternatives Modification

In this method, a new modification of the method of directed alternatives enumeration using the Kullback Leibler discrimination information is proposed for half-tone image recognition. Results of an experimental study in the problem of face images recognition with a large database are presented. It is shown that the proposed modification is characterized by increased speed of image recognition (5-10 times vs exhaustive search) [4].

# Chapter 2

# Problem Definition

The emerging need of image processing techniques in everyday life is inevitable. There have been lots of image processing algorithms proposed to increase the overall availability of tools in image understanding and using these tools to improve the human life. *Template Matching* is a task that its applications are obvious in everyday life. Computer vision tasks such as *object detection*, *object recognition* and other tasks based on these two main questions; Is there a certain object in the image? And if yes, where is it in the image?, can be classified as subproblems of *template matching* task. This task can be extended to counting the number of occurrences of an object in a given image. Given a main image and a template image, we want to find occurrences of the template image in main image. This problem can be solved in many ways. In the next chapter, we'll analyze the procedure of *naive* template matching to solve this problem. In further chapters, we'll provide the procedure of using *Fast Fourier Transform* to convert the images into frequency domain. We'll show that finding the maximum value of the result of the convolution of two images is where the template has occurred in main image.

## 2.1 Naive Template Matching

The main task of naive template matching was clearly explained in the previous section. There are various similarity measures in naive template matching. The one we use here is *SAD* or *Sum of Absolute Deviations* which is formally described further. Let $f$ and $t$ be the main image and the template image respectively and $(x, y)$ represent the column and the row of each image. The *Sum of Absolute Deviations* error metric for two images can be

written as:

$$SAD = \sum_{x,y} f(x,y) - t(x-u, y-v) \tag{2.1}$$

Note that there is also a more precise error metric called *Sum of Squared Errors* which is represented as:

$$SSD = \sum_{x,y} [f(x,y) - t(x-u, y-v)]^2 \tag{2.2}$$

In this project, we'll use the first error metric because of the processing power limits.

## 2.2 FFT-Based Template Matching

### 2.2.1 One-Dimensional Discrete Fourier Transform

The Fourier transform of a discrete function of one variable, $f(x)$, $x = 0, 1, 2, ..., M-1$, is given by the equation

$$F(u) = \frac{1}{M} \sum_{x=0}^{M-1} f(x) e^{-j2\pi ux/M} \qquad u = 0, 1, 2, ..., M-1 \tag{2.3}$$

Similarly, given $F(u)$, we can obtain the original function back using the inverse DFT:

$$f(x) = \sum_{u=0}^{M-1} F(u) e^{j2\pi ux/M} \qquad x = 0, 1, 2, ..., M-1 \tag{2.4}$$

### 2.2.2 Two-Dimensional Discrete Fourier Transform

Extension of the one-dimensional discrete Fourier transform and its inverse to two dimensions is straightforward. The discrete Fourier transform of a function (image) $f(x,y)$ of size $M * N$ is given by the equation

$$F(u,v) = \frac{1}{MN} \sum_{x=0}^{M-1} \sum_{y=0}^{N-1} f(x,y) e^{-j2\pi(ux/M + ry/N)} \tag{2.5}$$

As in the 1-D case, this expression must be computed for values of $u = 0, 1, 2, ..., M-1$, and also for $v = 1, 2, ..., N-1$. Similarly, given $F(u,v)$, we obtain $f(x,y)$ via the inverse Fourier transform, given by the expression

$$f(x,y) = \sum_{u=0}^{M-1} \sum_{r=0}^{N-1} F(u,v) e^{j2\pi(ux/M + ry/N)} \tag{2.6}$$

### 2.2.3 Convolution and Correlation Theorems

The discrete convolution of two functions $f(x, y)$ and $h(x, y)$ of size $M * N$ is denoted by $f(x, y) \star h(x, y)$ and is defined by the expression

$$f(x, y) \star h(x, y) = \frac{1}{MN} \sum_{m=0}^{M-1} \sum_{n=0}^{N-1} f(m, n) h(x - m, y - m) \tag{2.7}$$

we also know that the convolution theorem consists of the following relationships between the two functions and their Fourier transforms:

$$f(x, y) \star h(x, y) \leftrightarrow F(u, v) H(u, v) \tag{2.8}$$

and

$$f(x, y) h(x, y) \leftrightarrow F(u, v) \star H(u, v) \tag{2.9}$$

The correlation of two functions $f(x, y)$ and $h(x, y)$ is defined as

$$f(x, y) \circ h(x, y) = \frac{1}{MN} \sum_{m=0}^{M-1} \sum_{n=0}^{N-1} f^*(m, n) h(x + m, y + n) \tag{2.10}$$

where $f^*$ denotes the complex conjugate of $f$. Convolution is the tie between filtering in the spatial and frequency domains. The principal use of correlation is for matching. In matching, $f(x, y)$ is an image containing objects or regions. If we want to determine whether $f$ contains a particular object or region in which we are interested, we let $h(x, y)$ be that object or region (we call this image a template). Then, if there is a match, the correlation of two functions will be maximum at the location where $h$ finds a correspondence in $f$. An example of this phenomenon is provided in figure 2.1.

## 2.3 Fast Fourier Transform

One of the main reasons that the DFT has became an essential tool in signal processing was the development of the fast Fourier transform. Computing the 1-D Fourier transform of $M$ points requires on the order of $M^2$ multiplication/addition operations. The FFT accomplishes the same task on the order of $M \log_2 M$ operations. If, for example $M = 1024$, the brute-force method will require approximately $10^6$ operations. While the FFT will require approximately $10^4$ operations. This is a computational advantage of 100 to 1. The decrease in computational complexity significantly impacts the time needed for processing the images. The FFT algorithm is based on the so-called *successive doubling method*. Let's define the equation

$$F(u) = \frac{1}{M} \sum_{x=0}^{M-1} f(x) W_M^{ux} \tag{2.11}$$

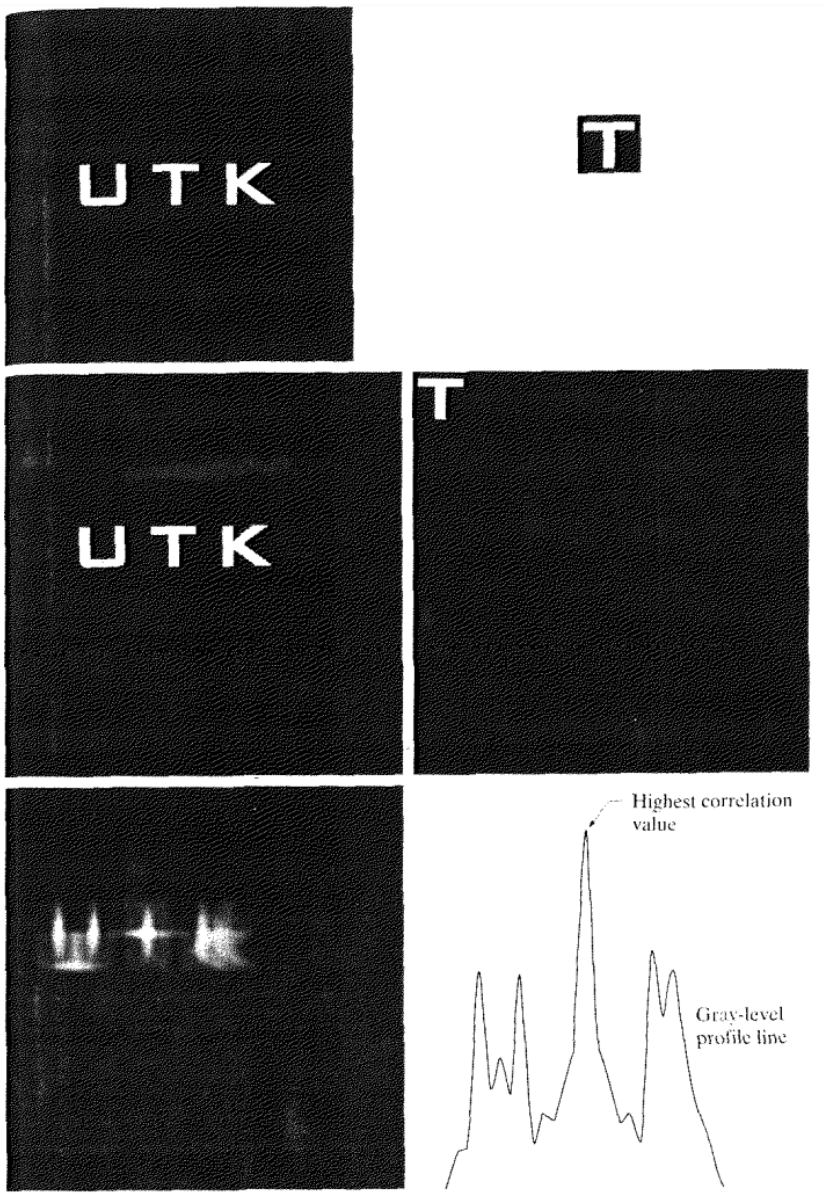


Figure 2.1: Illustration of image padding and correlation. The highest value of the correlation function occurs at the point where template is exactly on top of the $T$ in the image.

where

$$W_M = e^{-j2\pi/M} \tag{2.12}$$

and $M$ is assumed to be of the form

$$M = 2^n \tag{2.13}$$

with $n$ being a positive integer. Hence, $M$ can be expressed as

$$M = 2K \tag{2.14}$$

Substitution of (2.14) into (2.11) yields

$$F(u) = \frac{1}{2}[\frac{1}{K}\sum_{x=0}^{K-1} f(2x)W_{2K}^{u(2x)} + \frac{1}{K}\sum_{x=0}^{K-1} f(2x+1)W_{2k}^{u(2x+1)}] \tag{2.15}$$

The number of multiplications and additions required to implement FFT:

$$m(n) = 2m(n-1) + 2^{n-1} \quad n \geq 1 = \frac{1}{2}M\log_2 M \tag{2.16}$$

and

$$a(n) = 2a(n-1) + 2^n \quad n \geq 1 = M\log_2 M \tag{2.17}$$

# Chapter 3

# Implementation and Performance Analysis

## 3.1 Analysis of Naive Template Matching

In this section, we'll analyze the implementation and the performance of the *Naive Template Matching* algorithm. First of all, let's consider the serial implementation case.

### 3.1.1 Bitmap Images

For this project, we've used the *bitmap* image library by *Arash Partow* which is accessible here.

### 3.1.2 Serial Implementation of NTM

The serial implementation of this algorithm consists of 2 main loops to iterate over image pixels. There is also a need for each pixel we are iterating through, to calculate the *Sum of Absolute Deviations* which is the similarity measure between the main image pixels and the template image. Please refer to the *Naive Template Matching* algorithm to see the code. Since the task is mainly focused on counting the number of occurance inside the main images, we can obtain this by finding the minimum value of *SAD* while iterating through the main image pixels and counting the number of occurrences of the found minimum inside the main image matrix.

### 3.1.3 Timing the Serial NTM

We can obtain the elapsed time for the serial iteration using the *chrono* library. The code for this section is provided here. Please refer to the serial implementation code for the details.

### 3.1.4 CUDA Implementation of NTM

In this section we'll walk through the kernel codes provided in the *kernel.cu*.

#### Compute Sad Array Kernel

The image data is being stored in an 1-D array. Thus, the best choice for CUDA kernel launch parameters would be to set grid dimensions as $(image\_width/block\_size\_x, image\_height/block\_size\_y, 1)$. The main purpose of this choice is not the way we have stored the data, it actually depends on the input data. Since we are dealing with images it is more suitable to have 2-D blocks of threads. Further explanations focus on the kernel implementation. Initially, each thread finds its own global 2-D identification as rows and columns. Then, each thread virtually sees a kernel (template) around it self. This is the core of the parallelization section. All threads can see all of the iterations in one place. We then compute the SAD of each pixel and load it inside an SAD array. The next section describes the reason to do so.

#### Find Minimum in Array Kernel

We can obtain the best possible match by finding the minimum SAD in SAD array. We'll do so using shared memory to speed up the process. Each thread helps loading the data inside a block into the shared memory of that block. We then use *fminf* to find the minimum inside each block. Since we are using the shared memory, we need to do a *reduction* to find the minimum across different blocks. We can obtain this reduction task defining a *mutex* to control the global memory write by first thread of each block.

#### Find Number of Occurrences

Since the main task is to find the number of occurrences of template image in main image, we should count the number of occurrences of minimum SAD in the SAD array. To speed up the process we've used shared memory again. The intuition of using shared memory is exactly the same as the previous section.

### 3.1.5 Launch Parameters on Test Cases

The test has been done on three different sizes of images. One of the medium sized images is a *bitmap* image with dimensionality of $1112 * 1500$. The template image is a $116 * 116$ image in this case. Considering a block size of 1024 on a *Nvidia 850m GTX* (compute capability of 5), the launch parameters are provided below:

| | X | Y | Z |
|---|---|---|---|
| Grid Dimensions | 38 | 47 | 1 |
| Block Dimensions | 32 | 32 | 1 |

### 3.1.6 Occupancy Analysis

Before getting into the details, it is important to mention that maximum number of active warps in theory is 64. *Nsight* profiler provides great details on the number of active warps per SM. In this case, there are 63.83 active warps on the first kernel (Compute Sad Array Kernel). The occupancy can obtained by dividing the number of active warps to the number of maximum warps available:

$$occupancy = \frac{63.83}{64} = 99.74\% \tag{3.1}$$

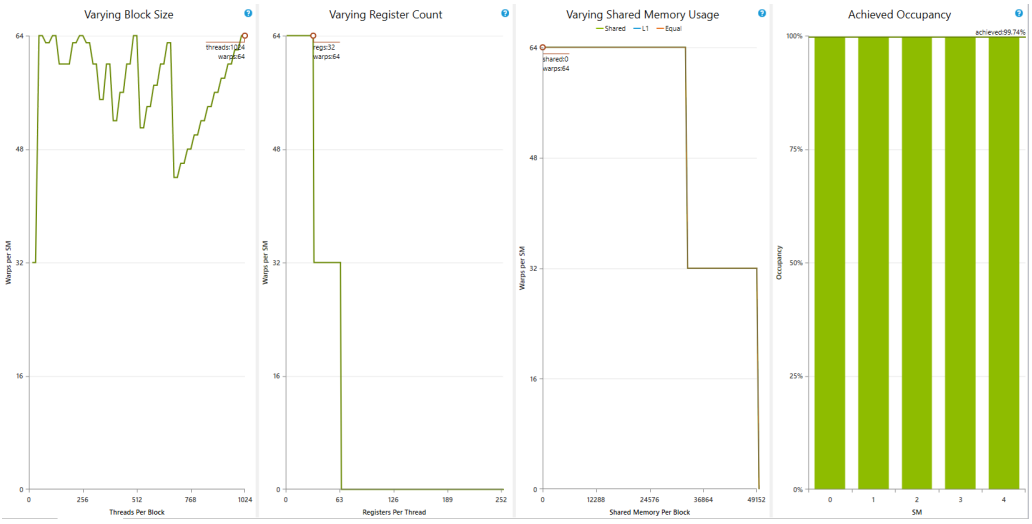


Figure 3.1: Illustration of varying the size of blocks, registers and shared memory on the achieved occupancy.

According to figure 3.1, varying the number of threads per block might yield the same result in other scenarios. The circled point shows the current number of threads per block and the current upper limit of active warps. Note that the number of active warps is not the number of warps per block (that is threads per block divided by warp size, rounded up). If the chart's line goes higher than the circle, changing the block size could increase occupancy without changing the other factors. Also, increasing the number of variables (registers per block) will drastically decrease the occupancy of the first kernel.

### 3.1.7 SM Activity Analysis

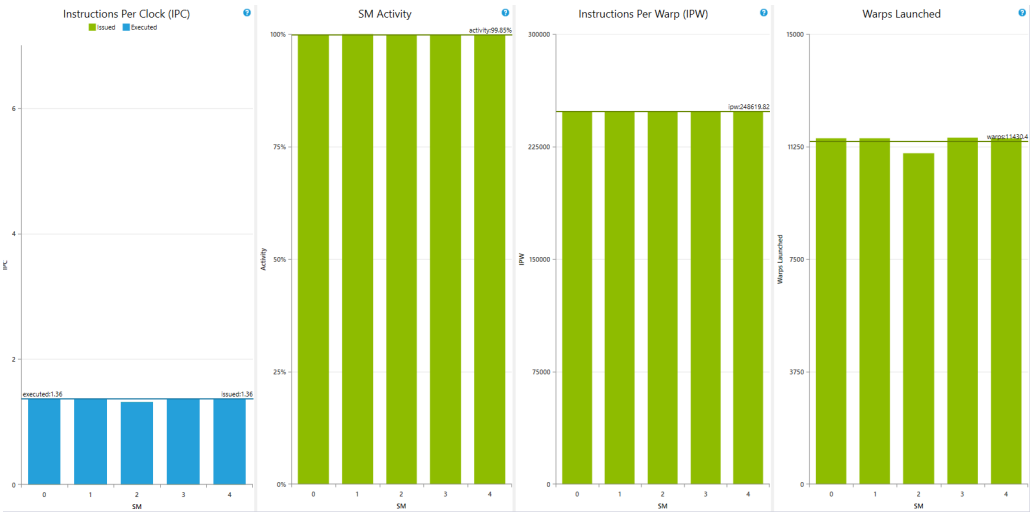


Figure 3.2: Issue efficiency and SM activity charts for the first (bottleneck) kernel.

The IPC chart demonstrates the achieved instructions throughputs per SM for both, issued instructions and executed instructions. The theoretical maximum peak IPC is a device limit and defined by the compute capabilities of the target device.

#### Issued IPC

The average number of issued instructions per cycle accounting for every iteration of instruction replays. Optimal if as close as possible to the Executed IPC. As described in the background section of this document, some assembly instructions require to be multi-issued. Hence, the instruction mix affects the definition of the optimal target for this metric. In this case, the issued

IPC throughput is minimum since there weren't any multi issue instructions in the first kernel.

#### Executed IPC

The average number of executed instructions per cycle. Each warp scheduler of a multiprocessor can execute instructions independently, a target goal of executing one instruction per cycle means executing on average with an IPC equal to the number of warp schedulers per SM. The maximum achievable target IPC for a kernel is dependent on the mixture of instructions executed.

#### SM Activity Chart

The second chart provides information on the activity of each SM during the kernel launch. A multiprocessor is considered to be active if at least one warp is currently assigned for execution. An SM can be inactive - even though the kernel grid is not yet completed - due to high workload imbalances. Such uneven balancing between the SMs can be caused by a few factors: Different execution times for the kernel blocks, variations between the number of scheduled blocks per SM, or a combination of the two. In this case, non of the above has occurred and the activity result is almost 100%.

#### IPW Chart

One of the most common patterns for varying IPWs is conditionally executed code blocks. IPW can be useful while having variations in SM activity chart which in this case, non of these have occurred.

### 3.1.8 Speedup Analysis

In this section, we'll analyze the possible theoretical speedup. For this purpose, we'll calculate the serial computation time for the *collection* and *collection_coin* images as described above. This table describes the average speedup of parallel naive template matching algorithm compared to serial implementation. As can be seen in the figure 3.3, the speedup obtained on GPU is dedicated to many different parameters. In order to calculate the theoretical speedup a direct use of *Amdahl's law* doesn't fit in this problem. One might say that the number of cores in this case is $N$ (Same as the number of threads), but GPU does not have as many physical cores as the number of threads that can be launched. Additionally, significant portion of kernel time is begin spent just waiting for the data to be *read/written* from/to global memory. Also, the frequency and operational power of CPU

cores is higher than GPU cores. In this section, we'll use a modified version of the Amdahl's law [**?**]:

$$S = \frac{1}{(1-p) + (k * p/N)} \qquad k = freq(CPU)/freq(GPU) \tag{3.2}$$

The core frequency of my Intel 4710HQ processor is 3490 MHz. The core frequency of each GPU core is 902 MHz. These information are extracted using beloved *CPU-Z* and *GPU-Z* programs. Replacing these information into 3.2 yields

$$S = \frac{1}{(1-p) + 3.86 * p/N} \tag{3.3}$$

since the size of input is constant in this law, we'll assume that 3.3 is correct for the third experiment. Let's suppose that $\frac{1}{4}$ of the main program is parallelized, thus $p = \frac{1}{4}$ and the number of threads to run is 1828864 (1786 blocks of 1024). Theoretical speedup will be

$$S = \frac{1}{(\frac{3}{4}) + 3.86 * \frac{\frac{1}{4}}{1828864}} = 1.33 \tag{3.4}$$

| | **Exp 1** | **Exp 2** | **Exp 3** | **Exp 4** |
|---|---|---|---|---|
| *Image * Template* | (630 * 459) * (116 * 116) | (1203 * 460) * (116 * 116) | (1211 * 1500) * (116 * 116) | (3840 * 2160) * (214 * 214) |
| *Serial NTM* | 10787 msec | 22615 msec | 92204 msec | 1722131 msec |
| *Parallel NTM* | 339 msec | 644 msec | 1975 msec | 27983 msec |
| *Parallel NTM + Data Transfer* | 345 msec | 665 msec | 1980 msec | 28977 msec |
| *Achieved Speedup* | ***31.82*** | ***35.11*** | ***46.68*** | ***61.54*** |

Figure 3.3: Computation and data transfer time for naive serial and parallel implementation.

### 3.1.9 Performance Analysis

In this section, we'll analyze the performance of the *Compute Sad Array Kernel*. Firstly, lets find the arithmetic intensity of this kernel. Arithmetic intensity $I$, also called *operational intensity*, is the ratio of *arithmetic operations* or *work* ($W$), to the *memory traffic* ($Q$) [**?**]:

$$I = \frac{W}{Q} \tag{3.5}$$

and denotes the number of operations per byte of memory traffic. When the work is represented as *FLOPS*, the arithmetic intensity will be *FLOPS/Byte*.

According to the *Naive Roofline Model*, the *attainable performance* is bound either by the *peak performance* or *memory bandwidth * arithmetic intensity*. In this case, the operational intensity can be obtained by following the memory access patterns and the work being done in the main kernel: It is given

| Statement | *Operations* | *# Global Memory Writes * bytes* | *# Global Memory Reads* bytes* | *# Constant Memory Reads* bytes* | *# Shared Memory Reads* bytes* |
|---|---|---|---|---|---|
| *row, col* | ()()()(* + * +) | 0 | 0 | 0 | `6 * sizeof(int)` |
| *1st conditional* | ()()(< <)() | 0 | 0 | `2 * sizeof(int)` | 0 |
| *1st loop* | ()()(<)() | 0 | 0 | `1 * sizeof(int)` | 0 |
| *2nd loop* | ()()(<)() | 0 | 0 | `1 * sizeof(int)` | 0 |
| *m_r* | ()()(*)()+ + + * + | 0 | `1 * sizeof(unsigned char)` | `1 * sizeof(int)` | 0 |
| *m_g* | ()()(*)()+ + + * + | 0 | `1 * sizeof(unsigned char)` | `1 * sizeof(int)` | 0 |
| *m_b* | ()()(*)()+ + + * + | 0 | `1 * sizeof(unsigned char)` | `1 * sizeof(int)` | 0 |
| *t_r* | ()()(*)() + * + | 0 | `1 * sizeof(unsigned char)` | `1 * sizeof(int)` | 0 |
| *t_g* | ()()(*)() + * + | 0 | `1 * sizeof(unsigned char)` | `1 * sizeof(int)` | 0 |
| *t_b* | ()()(*)() + * + | 0 | `1 * sizeof(unsigned char)` | `1 * sizeof(int)` | 0 |
| *SAD Write conditional* | ()()(*<)() + | `1 * sizeof(int)` | 0 | `1 * sizeof(int)` | 0 |
| **Final Operational Intensity** | 5 / (6 * sizeof(unsigned char) + 1 * sizeof(int) = 0.5 | | | | |
| **Nvidia 850m GTX DDR Bus Frequency** | 1001 MHz | | | | |
| **Nvidia 850m GTX DDR Bus Bandwidth** | 2 * 128 = 256 bits | | | | |
| **Nvidia 850m GTX Memory Bandwidth** | 32 GB/s | | | | |

Figure 3.4: Calculation of first kernel operational intensity and GPU memory bandwidth.

that the *single precision* processing power of a *Nvidia 850m GTX* is 1155 GFLOPS [**?**]. Given these results, the kernel is actually memory bound since $0.5 < 1155/32 = 36$. The kernel arithmetic intensity should be at least 36 to be considered a compute bound kernel.

## 3.2 Implementation of FFT Based Template Matching

In this section, we delve into the details of *FFT* based template matching using *cufft* library from *Nvidia*. Note that this implementation is still in progress and there are multiple serial loops conducted in preprocessing step which slows down the process compared to the *naive template matching* procedure. As mentioned before, the overall procedure is to convert the spatial domain of input images to the frequency domain. In the frequency domain, we can apply a correlation based operation. This operation yields a signal of the same size as main image size. We then apply an inverse Fourier transform to turn the results back to the spatial domain. We then find the maximum of that signal and the number of occurrences of that maximum value in that

signal. The procedure is well defined below[**?**]:

$$c = real(IFFT_{2D}(FFT_{2D}(main\_image).*FFT_{2D}(template\_image))) \quad (3.6)$$

according to 3.6, $c$ contains a list of values which we are desired to find the maximum of it (for maximum similarity). To obtain this in CUDA, we've used multiple functions which are described further. Note that * symbol shows the complex conjugate of the second signal.

### 3.2.1 Real to Complex Conversion

For this part, we have not focused on the performance. We use simple *for* loops to convert the image data matrix to the proper format of *cufft* library which is called *cufftComplex*. *cufftComplex* is a simple typedef of *float* type in C.

### 3.2.2 Padding Data

Before performing a *2-D Forward Fourier Transform* we are urged to perform a data padding on template signal to make it the same size as the main signal. Figure 2.1 illustrates this phenomenon pretty well. The duty of data padding is simple. Allocate new memory with a new size. Copy signals into their corresponding location in new allocated memory and set other places to 0.

### 3.2.3 2-D FFT Planning

*cufft* library uses the concept of *plan* to provide the baseline setup for the main APIs provided in the library. A plan can initiate a 1-D, 2-D or 3-D data processing API from *cufft* library. In this implementation, we need a setup for a 2 dimensional Fourier transform, thus we use *cufftPlan2d* to prepare the library for the main transformations.

### 3.2.4 Forward FFT Launch

In order to launch a forward *complex to complex* Fourier transform using *cufft*, we'll use *cufftExecC2C*. The constant *CUFFT_FORWARD* shows the direction of the Fourier transform which is *Forward* in this case.

### 3.2.5 Complex Conjugate Kernel

This kernel implements the conjugation procedure. The implementation is pretty straightforward. Each thread multiples the corresponding signal point's complex part to -1 and loads it back to the input signal.

### 3.2.6 Complex Point-wise Kernel

This kernel provides a point to point multiplication manner for each of the points in main and template input signals. It uses another kernel called *ComplexMul* to perform a *complex multiplication*. It then scales the result using *ComplexScale*. Scaling or normalization is mainly done by dividing the signal values to the size of the signal.

### 3.2.7 Inverse FFT Launch

Finally, we'll perform an inverse Fourier transform on the result of the *Complex Point-wise Kernel*. The resulting signal is in the spatial domain.

### 3.2.8 Maximum Value and Number of Occurrences

To find the number of occurrences, we *serially* iterate over the resulting signal of the previous section. Note that these steps are not *100%* efficient and are still in improvement.

# Chapter 4

# Future Work

We admit the possible drawbacks and inefficiencies existing in this project, thus we have the following key improvement to-do list:

- Reorganization of the project structure, header files and .c files.
- Reorganization of the project source code for a C unified implementation.
- Usage shared memory techniques to improve the performance of the *NTM* implementation.
- Usage of highly-optimized image libraries such as *OpenCV* for *image rotation*, *image matrix extraction* and general *bitmap processing*.
- Implementation of CUDA kernels for real-to-complex signal conversions.
- Implementation of CUDA kernel to find the number of occurrences of template signal in main signal in *Fourier* based template matching.

# Chapter 5

# Conclusion

In this project, we analyzed various algorithms for the task of *Image Template Matching*. It is fair to say that there are already highly optimized libraries with template matching capabilities such as *OpenCV*, but as mentioned before, the main purpose of this project is to improve the understanding of the CUDA environment and parallel implementation of highly-demanded computer vision tasks such as template matching. We analyzed two main methods to perform this task:

1. Naive Template Matching
2. FFT Based Template Matching

For further read, please refer to methods such as *Stereo Matching*, *Image Registration* and *Scale Invariant Feature Transform*.

# References

[1] Tan, Xiaoyang, et al. Face Recognition from a Single Image per Person: A Survey. Pattern Recognition, vol. 39, no. 9, 2006, pp. 17251745.

[2] Beis, Jeffrey S., and David G. Lowe. "Shape indexing using approximate nearest-neighbour search in high-dimensional spaces." cvpr. IEEE, 1997.

[3] Savchenko, Andrey V. "Real-time image recognition with the parallel directed enumeration method." International Conference on Computer Vision Systems. Springer, Berlin, Heidelberg, 2013.

[4] Savchenko, Andrey V. Image Recognition with a Large Database Using Method of Directed Enumeration Alternatives Modification. RSFDGrC11 Proceedings of the 13th International Conference on Rough Sets, Fuzzy Sets, Data Mining and Granular Computing, 2011, pp. 338341.